**ORIGINAL ARTICLES**

Division of Pharmaceutics[1], Faculty of Pharmacy, Rhodes University, Makhanda; Aspen Pharmacare[2], Woodmead, Gauteng, South Africa

# Preformulation studies of efavirenz with lipid excipients using thermal and spectroscopic techniques

P. A. Makoni[1], K. W. Kasongo[1,2], R. B. Walker[1,*]

Investigation and identification of potential lipids for the manufacture of efavirenz loaded solid lipid nanoparticles (SLN) and nanostructured lipid carriers (NLC) was undertaken. Polymorphic modification and characteristics of the lipids with the best solubilising potential for efavirenz was explored using Fourier Transform Infrared Spectroscopy (FT-IR), Differential Scanning Calorimetry (DSC) and Wide-angle X-ray Scattering (WAXS). Lipid screening revealed that EFV is highly soluble in solid and liquid lipids, with glyceryl monostearate (GM) and Transcutol® HP (THP) exhibiting the best solubilising potential for EFV. GM exists in a stable β-polymorphic modification prior to exposure to heat, but exists in an α-polymorphic modification following exposure to heat. However, it was established that the addition of THP to GM revealed the co-existence of the α- and β'-polymorphic modifications of the lipid. EFV (60% *w/w*) exists in a crystalline state in a 70:30 mixture of GM and THP. Investigation of binary mixtures of EFV/GM and GM/THP, in addition to eutectic mixtures of EFV, GM and THP using FT-IR, DSC and WAXS revealed no potential interactions between EFV and the lipids selected for the production of the nanocarriers.

## 1. Introduction

The Human Immunodeficiency Virus (HIV) is known to cause Acquired Immune Deficiency Syndrome (AIDS) (Ravichandran et al. 2008). AIDS remains a serious cause for concern throughout the world. In 2017, 36.9 million people were reported to be living with HIV worldwide, among them 1.8 million children under 15 years of age. During the same year 35.4 million deaths worldwide were attributed to AIDS-related illnesses since the start of the epidemic (UNAIDS, n.d.).

Efavirenz (EFV), a non-nucleoside reverse transcriptase inhibitor (NNRTI) is used for highly active antiretroviral therapy (HAART) to treat HIV-1 infection in adults, adolescents and children. EFV was approved by the United States Food and Drug Administration (FDA) in September 1998 (Bozal et al. 2011; Médecins Sans Frontières Access Campaign, n.d.; Ravichandran et al. 2008). EFV is used with other antiretroviral medicines for the treatment of HIV-1 infected adults, adolescents and children weighing > 13 kg and/or older than 3 years (Rossiter and University of Cape Town. Division of Clinical Pharmacology, 2016).

EFV is a Biopharmaceutical Classification System (BCS) Class II compound of low aqueous solubility and high intestinal permeability (Taneja et al. 2016). EFV is lipophilic and is highly protein bound to albumin (~99.5–99.75%). It has a high affinity for human adipose tissue due to its lipophilic nature (Almond et al. 2005; Dupin et al. 2002). However psychiatric effects, such as severe depression and suicidal ideation have been reported in patients treated with EFV, due to high EFV levels in the CNS from associated "dose-dumping" when using conventional oral dosage forms. This ultimately leads to discontinuation of this potent, durable and relatively simple addition to HAART (Makoni et al. 2019; Puzantian 2002). Effective entrapment of EFV into novel colloidal delivery systems such as solid lipid nanoparticles (SLN) and/or nanostructured lipid carries (NLC), for oral administration, may sustain the release of EFV thus slowing the rate of absorption and potentially modulating bioavailability, so as to reduce the incidence of adverse psychiatric effects. SLN and NLC have the advantage of sustaining drug release to maintain constant plasma levels in addition to bypassing the reticuloendothelial system making them suitable as delivery systems that can target the brain (Ghasemiyeh and Mohammadi-Samani 2018).

SLN and NLC are innovative lipid carriers used to form a matrix of biocompatible lipid(s) that remain in the solid state at room and body temperature with a mean particle size ranging between 10 and 1000 nm. SLN are manufactured using lipids that are solid at room and body temperature stabilised using one or more surfactant(s) (Wissing et al. 2004). NLC have similar physicochemical properties to SLN with a nano-structured architecture of the lipid matrix in order to increase API loading, whilst preventing API leakage on storage, thereby resulting in greater flexibility for targeting specific release profiles (Hu et al. 2006; Souto and Müller 2011). The structural matrices of NLC are derived from a mixture of solid and liquid lipids that are used in specific ratio combinations, resulting in a less ordered lipid matrix with numerous imperfections that accommodate a larger amount of API. NLC particles solidify on cooling but do not recrystallise and remain in an amorphous state (Müller et al. 2002; Müller et al. 2002; Souto et al. 2004; Souto and Müller 2011). API expulsion on prolonged storage is less likely to occur from NLC as compared to SLN due to the differences in architecture of the lipid matrices. Due to the lipid-based nature of SLN and NLC, their popularity has developed rapidly due to biocompatibility and biodegradability, formulation and manufacturing flexibility using well-characterised generally regarded as safe (GRAS) excipients (Mehnert and Mäder 2002; Souto and Müller 2011).

These studies aimed to identify and characterise solid and liquid lipids for the formulation and preparation of EFV-loaded SLN and NLC for oral use, with the primary aim of controlling the rate of EFV release, thus attempting to minimise the psychiatric side effects associated with the use of this molecule.

## 2. Investigations, results and discussion

### 2.1. Selection of lipids

The solubility of EFV in the lipids used was essential to establish prior to the development and optimisation of SLN/NLC. The usefulness of SLN and/or NLC as carrier systems for an API is dependent on loading capacity (LC) and encapsulation efficiency (EE) of the nanoparticles for a particular API (Souto and Müller 2011) and a major factor that affects the LC and EE of SLN and/or NLC for an API, is the solubility of that API in molten lipid (Hou et al. 2003; Müller et al. 2000; Wissing et al. 2004). An adequate LC and EE can be achieved only when the solubility of the API in molten lipid is relatively high (Hou et al. 2003; Müller et al. 2000; Wissing et al. 2004). Consequently, it is important to evaluate the solubility of EFV in different solid and liquid lipids, with the primary aim of identifying a solid and/or liquid lipid combination with the best solubilising potential for EFV, in this case. Solubility data are graphically depicted in Fig. 1.
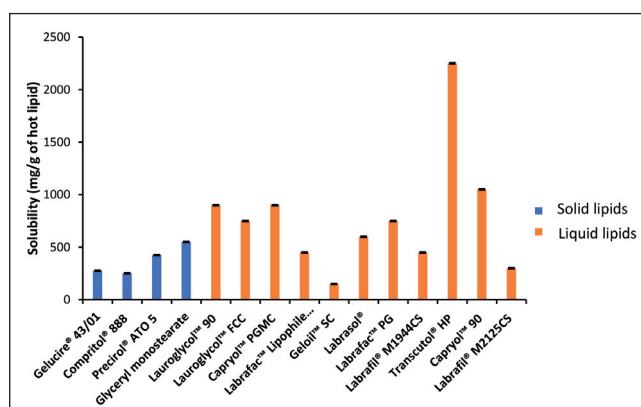


Fig. 1: Solubility of EFV in 1.0 g of different solid and liquid lipids at 70 °C (n=3)

The data in Fig. 1 reveal that EFV is soluble to some degree in each of the lipids investigated. The solubility of EFV in glyceryl monostearate (GM) was the greatest observed for the solid lipids as the presence of mono- and diglycerides in lipid matrices promotes solubilisation of API (Müller et al. 2000). GM possesses oxygen and hydroxyl functional groups which have been shown to increase the polarity and hydrogen bonding possibilities of the compound (Makoni et al. 2020), thereby resulting in a possible increase in solubility of EFV. GM was used in formulation development activities in addition to optimization investigations of EFV-loaded SLN and NLC.

In contrast to SLN, the structural matrix of NLC requires the addition of a liquid lipid that results in the formation of less ordered lipid matrices with imperfections that ultimately may accommodate larger amounts of API (Hu et al. 2006; Souto and Müller 2011). The data depicted in Fig. 1 reveals that EFV is highly soluble in Transcutol® HP (THP), which is a combination of diethylene glycol monoethyl ethers. In addition, THP has two ester and hydroxyl functional groups which increases the polarity and hydrogen bonding possibilities of the compound (Makoni et al. 2020) resulting in an increase in the solubility of EFV in THP. Consequently, THP was selected as the liquid lipid for use in formulation development and optimization studies of EFV-loaded NLC.

The production of NLC involves mixing lipid molecules that are spatially different, viz. solid and liquid lipids, invariably resulting in the melting point of the solid lipid decreasing (Joshi and Patravale 2006; Müller et al. 2002; Kasongo 2010). It is ideal to incorporate a relatively large amount of oil into a solid lipid to improve the solubility of API and subsequently increase the loading capacity of the NLC for that API (Müller et al. 2002; Kasongo 2010). Nevertheless, NLC must remain solid at room and body temperatures and therefore as a general rule the melting point of the solid lipid to be used should be > 40 °C (Joshi and

Patravale 2006; Müller et al. 2002; Kasongo 2010) after combining with a liquid lipid and the solid lipid should be miscible with the liquid lipid to permit formation of imperfections in the crystal lattice structure of the solid lipid to facilitate API loading (Müller et al. 2008; Souto et al. 2006).

Glyceryl monostearate (GM) and Transcutol® HP (THP) were mixed in different ratios and exposed to a temperature of 70 °C for one hour and cooling to room temperature (22 °C). An aliquot of each sample was then smeared onto filter paper and the miscibility of the lipids assessed visually. The appearance of lipid on the filter paper was a clear indication of poor miscibility of the lipids and any binary mixture in which droplets were observed was considered unsuitable for use (Kasongo et al. 2011). The data are summarized Table 1.

Table 1: Visual observation data for assessment of miscibility of binary mixtures of GM and THP

| GM: THP | Visual observation |
|---------|--------------------|
| 95:5 | No oil droplets observed on filter paper |
| 90:10 | No oil droplets observed on filter paper |
| 85:15 | No oil droplets observed on filter paper |
| 80:20 | No oil droplets observed on filter paper |
| 75:25 | No oil droplets observed on filter paper |
| 70:30 | No oil droplets observed on filter paper |
| 60:40 | Oil droplets observed on filter paper |
| 50:50 | Oil droplets observed on filter paper |
| 40:60 | Oil droplets observed on filter paper |

The results revealed no THP droplets on the filter paper following incorporation up to 30% w/w level. Consequently, a 70:30 binary mixture of GM and THP was used in combination for the formulation and manufacture of EFV-loaded NLC. The 70:30 binary mixture had a melting onset of 49.32 °C. The maximum solubility of EFV in 1.0 g of the 70:30 binary mixture was visually determined to be 1.4 g (58.3% w/w). The addition of 1.5 g (60% w/w) resulted in attainment of saturation solubility.

### 2.2. Characterisation of selected lipids

#### 2.2.1. FT-IR

Qualitative FT-IR can be used for fingerprint identification of molecules and reveals potential interactions at a molecular level as functional groups exhibit unique molecular vibrations at specific frequencies (Venkatesham et al. 2012). The FT-IR spectra for GM prior to and following exposure to heat are depicted in Fig. 2. The FT-IR spectrum for GM revealed the presence of characteristic bands for the –OH functional group at a frequency of 3384 cm$^{-1}$, C-H stretching at 2950-2910 cm$^{-1}$ and an ester carbonyl group at
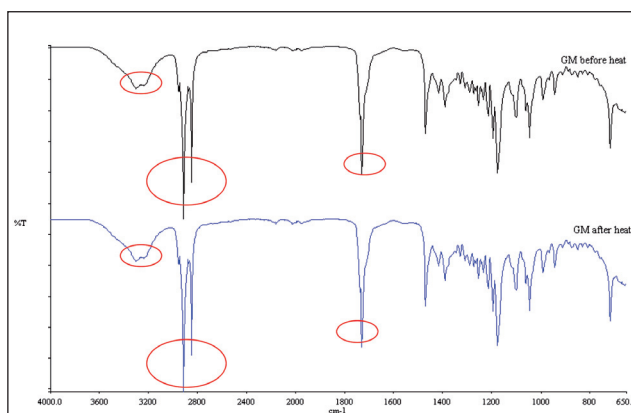


Fig. 2: FT-IR spectra of GM prior to and following exposure to 70°C for one hour.

1733 cm$^{-1}$ (Makoni 2014; Makoni et al. 2019). Following exposure to heat, the major band (circled) for GM did not change, indicating that no vibrational energy changes for the chemical bonds were observed suggesting no polymorphic or other changes had occurred following application of heat.

The FT-IR spectrum of GM and that of a 70:30 binary mixture of GM and THP following exposure to heat are depicted in Fig. 3. It is evident that both spectra reveal the presence of bands characteristic for GM (circled) and following incorporation of THP into GM no additional peaks were observed, confirming the lack of interaction between the liquid and solid lipid. However, a marked reduction in the intensity of the peaks was observed indicating the impact of dilution on the intensity of the molecular vibrations for GM following THP inclusion.
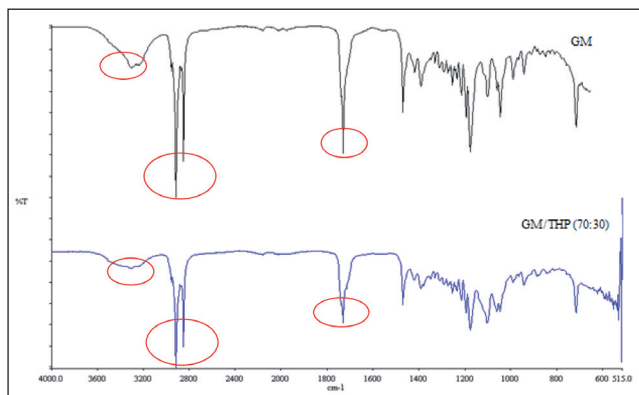


Fig. 3: FT-IR spectra for GM and a 70:30 binary mixture of GM and THP following exposure to 70°C for one hour.

The FT-IR spectrum of EFV and that of a 1:1 binary mixture of EFV and GM prior to heating is depicted in Fig. 4. These data reveal that there are additional peaks for GM in the binary mixture that occur at a frequency between 2950 and 2910 cm$^{-1}$ (circled in green) that correspond to a C-H bond stretch in the EFV molecule. The spectrum for the binary mixture also reveals other frequency bands characteristic of EFV (circled in red), confirming the absence of any interaction between EFV and GM in this binary mixture. However real time stability studies should be conducted to establish if this is indeed the case.

The FT-IR spectrum generated for EFV and GM prior to exposure to heat and that of a 1:1:1 ternary mixture of EFV, GM and THP following exposure to heat is depicted in Fig. 5. Evaluation of the FT-IR spectrum for the ternary mixture reveals the presence of peaks (circled in green) that are the same as those observed for GM, confirming that neither THP nor EFV interacts with the crystalline structure of GM. However, the absence of peaks representing molecular vibrations for EFV is probably a result of incorporation of EFV as a molecular dispersion in the ternary mixture that is supported by the solubility data reported in Section 2.1.
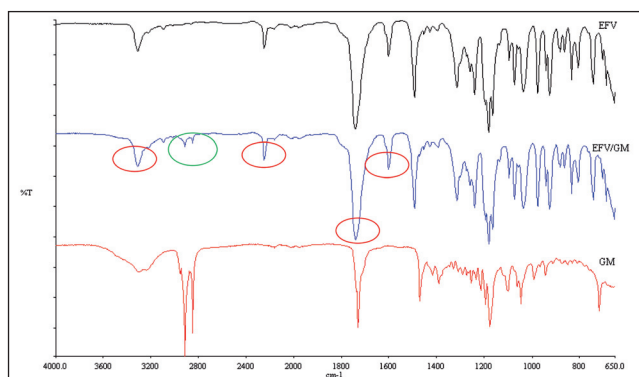


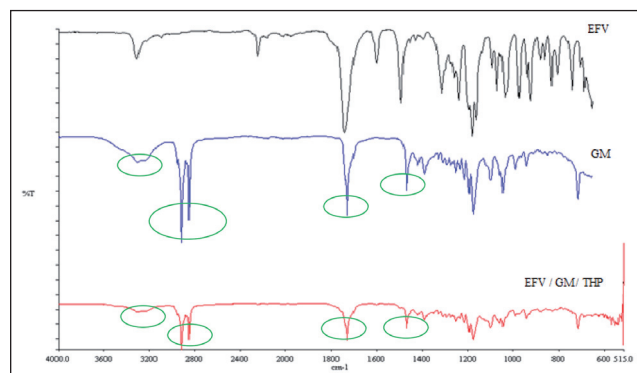Fig. 4: FT-IR spectra of EFV, GM and a 1:1 binary mixture of EFV and GM generated prior to heating.



Fig. 5: FT-IR spectra of EFV and GM prior to exposure to heat and a 1:1:1 mixture of EFV, GM and THP following exposure to 70°C for one hour.

### 2.2.2. DSC

DSC is used to explicate crystallisation and melting behaviour(s) of solids including lipid nanoparticles and operates on the principle that modifications and lipids will result in different melting points of different enthalpy (Mehnert and Mäder 2002; Venkatesham et al. 2012). Consequently, the crystalline nature and polymorphic modification of excipients was characterised using DSC. The DSC thermograms of GM generated prior to and following exposure to heat and GM after exposure to heat and a 70:30 binary mixture with THP following exposure to heat are depicted in Figs. 6 and 7 respectively.
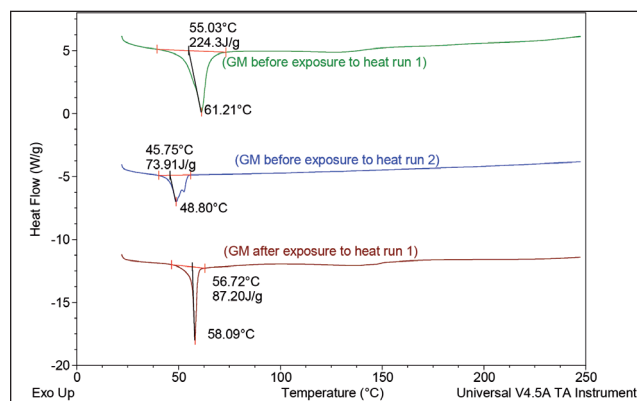


Fig. 6: DSC thermograms of glyceryl monostearate generated prior to and following exposure to 70 °C for one hour.
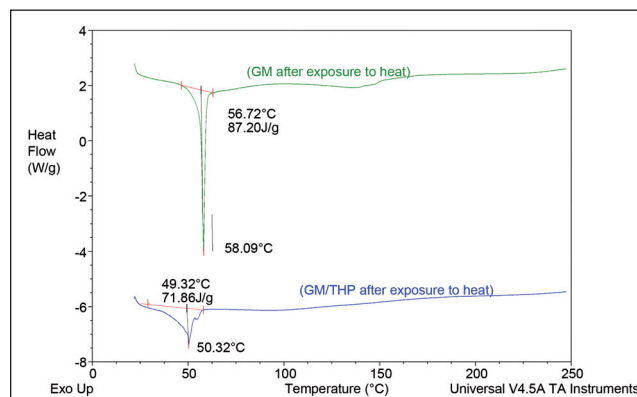


Fig. 7: DSC thermograms of GM and of a 70:30 binary mixture of GM and THP generated following exposure to 70 °C for one hour.

The thermogram generated prior to heating (run 1) (Fig. 6) reveals a single peak at an onset temperature and melting point of 55.03 °C and 61.12 °C respectively. This is consistent with presence of the β'-modification of GM (Zimmermann et al. 2005) and is

confirmation that the solid lipid exists as a single polymorphic form prior to exposure to heat. In addition, the data reveal that the melting enthalpy for the initial study was 224.3 J/g. This value is relatively high compared to those obtained for samples following exposure to DSC analysis for a second time (73.91 J/g) and a first run following exposure to heat of 87.20 J/g indicating that GM exists in a highly crystalline state prior to exposure to heat. The thermogram generated following a second DSC scan of the same sample of GM (run 2) reveals the presence of two peaks, with an onset temperature for the major peak reduced from 55.03 to 45.75 °C. The presence of two peaks may be attributed to the presence of β'- and α-modifications of GM (Müller et al. 2008). Therefore, it is clear that GM recrystallizes as two polymorphic forms following exposure to heat. It is also evident that the melting enthalpy following a second DSC scan of 73.91 J/g is lower than 224.3 J/g observed when the sample was subjected to a single DSC run suggesting that following exposure to an isothermal phase at 22 °C for 10 min, the lipid had not yet recrystallized to the preferred form.
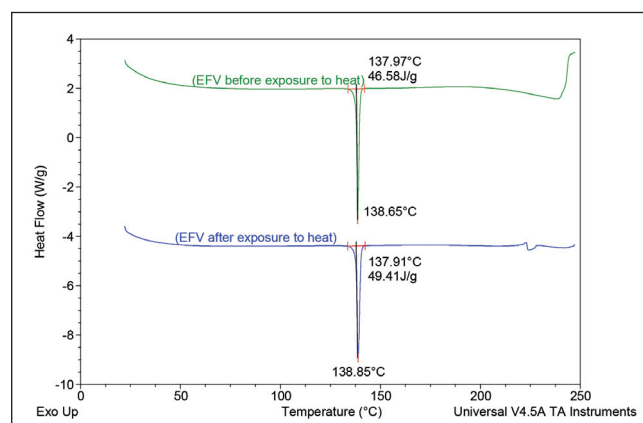


Fig. 8: DSC thermograms for EFV prior to and following exposure to 70 °C for one hour.

Exposure of GM to heat prior to DSC analysis once again revealed a single endothermic peak with an onset temperature and melting point of 56.72 °C and 58.09 °C respectively, revealing the presence of a single polymorphic form for GM. This can be attributed to the presence of the complete α-modification form of the compound. In addition, the low enthalpy of 87.20 J/g suggests a less crystalline lattice structure of GM in comparison to that observed for GM prior to exposure to heat (224.3 J/g), implying the presence of the α-modification.

Incorporation of THP into the mixture with GM resulted in changes to the polymorphic and crystalline nature of solid lipid (GM) and is depicted in Fig. 7 (Makoni et al. 2019). The DSC thermogram of a 70:30 binary mixture of GM and THP following exposure to heat revealed the presence of two discrete endotherms indicative of the co-existence of different polymorphs of GM. The melting onset of 49.32 °C observed for the major peak suggests the less crystalline α-modification is present and the minor peak the more crystalline β'-modification. The inclusion of THP into GM appears to create imperfections within the solid lipid matrix that consequently results in melting point reduction from 58.09 to 50.32 °C. The resultant binary mixture is also less crystalline in nature than GM alone, as confirmed by the decrease in enthalpy from 87.20 J/g to 71.86 J/g (Makoni et al. 2019).

The potential effects of temperature on the crystalline and polymorphic nature of EFV were determined prior to investigating the effect of incorporating EFV into GM or a binary mixture of GM/THP. The DSC thermogram for EFV prior to and after heating is depicted in Fig. 8 (Makoni et al. 2019).

The DSC data generated for EFV reveal the presence of a sharp single melting endotherm at 138.65 °C (enthalpy = 46.58 J/g) and 138.85 °C (enthalpy = 49.41 J/g) respectively. These data clearly indicate that EFV exists as a single polymorph and that the poly-

morphic nature of the molecule does not change following exposure to heat. The sharp nature and narrow peak width of 0.68 observed prior to exposure to heat reveal that EFV is a highly crystalline material. Following exposure to heat the peak width increases to 0.94, indicating that heating EFV may disrupt the crystal structure of the molecule to some extent. Nevertheless the peak observed in the thermogram is sharp, revealing the lack of a significant change in the crystalline nature of the molecule following exposure to heat (Makoni et al. 2019).

The DSC data for the binary mixture (0.6 g EFV in 1.0 g GM) and a ternary mixture of EFV/GM/THP (1.5 g EFV in 1.0 g, 70:30 GM:THP binary mixture) before and after heating were generated to verify the absence of an incompatibility between EFV and the selected lipids. The DSC thermograms are depicted in Figs. 9 and 10.
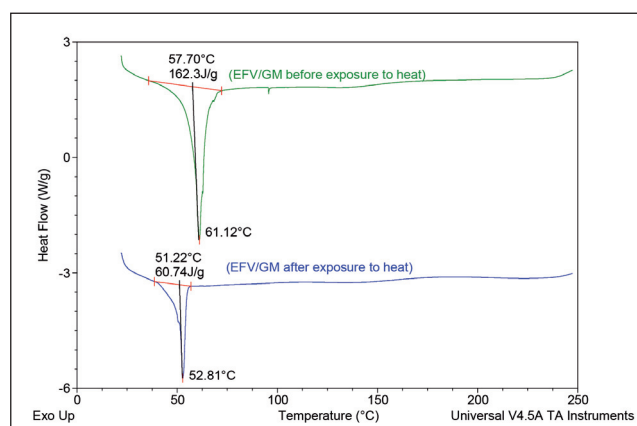


Fig. 9: DSC thermogram for a binary mixture of EFV and GM prior to and following exposure to 70 °C for one hour.
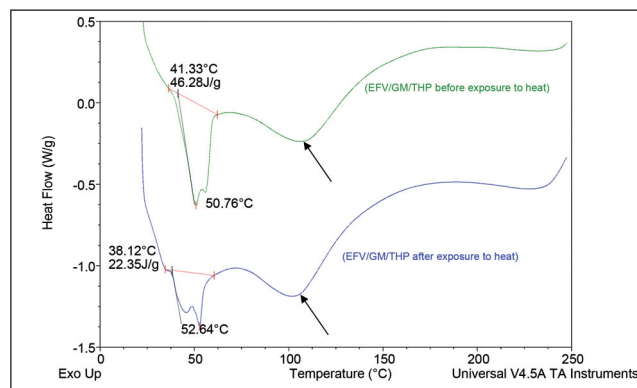


Fig. 10: DSC thermogram for a ternary mixture of EFV, GM and THP prior to and following exposure to 70 °C for one hour.

The DSC thermograms for the binary mixture (0.6 g EFV in 1.0 g GM) of EFV and GM prior to and following exposure to heat reveal the presence of a single peak due to melting of GM. This data reveals no evidence of an interaction between EFV and the solid lipid. However, the absence of a visible peak due for EFV in each thermogram indicates that EFV is largely dissolved in GM as the molecule is highly lipophilic and exhibits a high degree of solubility in GM. The DSC thermogram for the binary mixture of EFV and GM following exposure to heat revealed a peak with an onset temperature of 51.22 °C and an enthalpy of 60.74 J/g, which is a characteristic of the less crystalline α-modification of GM and not the crystalline β-modification with an enthalpy of 162.3 J/g.

The DSC thermogram generated for the ternary mixture (1.5 g EFV in 1.0 g, 70:30 GM: THP binary mixture) prior to and following exposure to heat clearly shows the presence of separate endothermic events consistent with those observed for GM and EFV. However, the melting event for EFV (identified with an arrow) in the ternary mixture that was exposed to heat was relatively

small compared to that observed for the ternary mixture prior to exposure to heat, which indicates that EFV is highly soluble in the molten lipid mixture. However, the presence of the peak for EFV in both thermograms is also indicative of the existence of EFV in a crystalline state, which is most probably a result of exceeding the saturation solubility of the molecule in the lipids, since 60% *w/w* EFV was used in these studies. The sample analysed following exposure to heat exhibited an enthalpy of 22.35 J/g, which is much lower than that of 46.28 J/g observed for the sample analysed prior to exposure to heat, indicating that heat exposure of the sample results in the formation of a less crystalline lattice allowing for further dissolution of EFV in the binary mixture.

### 2.2.3. WAXS

WAXS data was used to investigate the lamellar arrangement of lipid molecules and crystallinity of fatty acid acyl glycerol chains of GM. GM is a mixture of mono-, di- and tri-acyl glycerol (Rowe et al. 2009). Due to differences in chain length of the acyl glycerol fatty acids (palmitic and stearic acids) and the hydroxyl functional groups (3) of glycerol a β'-modification of the lipid occurs (Müller et al. 2008). The differences observed in the WAXS for GM prior to and following exposure to heat are evident from Fig. 11.
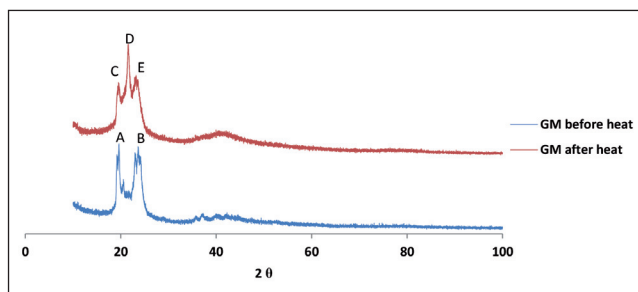


Fig. 11: WAXS patterns for glyceryl monostearate generated prior to (blue) and following (red) exposure to 70 °C for one hour.

Exposure of GM to heat leads to an increase in the intensity of peak A, that is a consequence of a drastic decrease in the crystallinity of the fatty acid side chains. The increase in peak intensity and decrease in side chain crystallinity can be attributed to heating that results in modification of the lamellar structure resulting in possible polymorphic transitions. The diffraction patterns reveal scattering peaks around peak A that permits the identification of lipid modifications (Kasongo et al. 2011; Müller et al. 2008). The Bragg spacing distances were calculated using (Eq. 1) and used to identify polymorphic modifications of GM prior to and following exposure to heat.
The WAXS for GM reveals two scattering reflections identified as A and B (Fig. 11) prior to heating, corresponding to Bragg distances of 0.420 and 0.385 nm respectively. This indicates that the highly crystalline β'-modification form is present and is consistent with the DSC data observed. WAXS patterns for GM generated following heating reveal the presence of three scattering reflections identified as C, D and E, corresponding to Bragg distances of 0.420, 0.461 and 0.398 nm respectively, which are indicative of the presence of a $\beta_i$-modification. However, DSC data suggest the presence of a single polymorph following exposure of GM to heat. The use of WAXS permitted identification of two additional scattering reflections however, the scattering reflection D, located at a Bragg spacing of 0.420 nm, was significantly greater in intensity than those observed for B and C and this result is consistent with the presence of the less crystalline α-modification form. The combination of DSC and WAXS information support the notion that exposure of GM to heat causes a change in the crystalline nature of the lipid and ultimately the polymorphic form in which it exists.
The WAXS patterns for a 70:30 binary mixture of GM and THP generated following exposure of the lipid mixture to heat is depicted in Fig. 12.
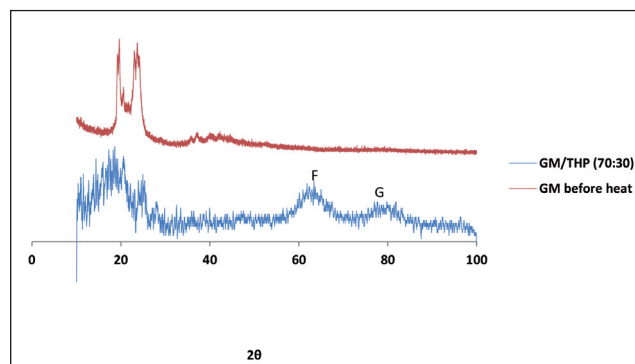


Fig. 12: WAXS patterns for a 70:30 binary mixture of GM and THP (blue) generated following exposure of the lipid mixture to 70 °C for one hour.

The WAXS for a 70:30 binary mixture of GM and THP following exposure to heat produced Bragg distances similar to that for GM alone, in addition to two reflections in the region 2θ = 60–85° *viz.*, F and G, suggesting that the lipid mixture produced occurs in the β-polymorphic form. DSC data revealed the co-existence of the α- and β'-polymorphic modifications which is likely to be the case, although WAXS did not detect the presence of the the α- polymorphic form, possibly due to the low intensity signal for the material in the diffractogram.
WAXS was used to identify potential interactions between EFV and the lipids to be used in the nano-particulate formulations. Similar to DSC studies, WAXS diffractograms of EFV prior to and following exposure heat were generated and used as a reference to identify potential interactions between EFV and the lipids.
The WAXS pattern for a binary mixture of GM and EFV (0.60 g EFV in 1.0 g GM) following heating and cooling is depicted in Fig. 13. The data for the diffraction patterns include a number of reflection signals that are consistent with those detected for EFV, indicating incomplete dissolution of the compound in GM for the ratios used for this study. However, the intensities of the peaks for EFV in the binary mixture following exposure to heat are significantly lower than those observed prior to exposure of the mixture to heat, which supports the notion that EFV dissolves in the molten lipid matrix.
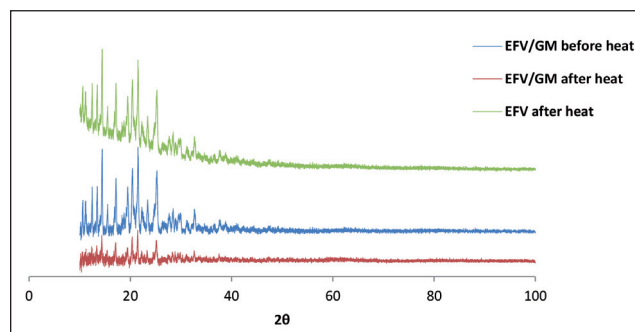


Fig. 13: WAXS patterns of a binary mixture of GM and EFV generated prior to (blue) and following exposure (red) to 70 °C for one hour.

The WAXS pattern generated for the ternary mixture of EFV, GM and THP (1.5 g EFV in 1.0 g, 70:30 GM: THP binary mixture) following exposure to heat, in addition to the WAXS pattern for EFV generated prior to exposure to heat is depicted in Fig. 14.
The WAXS diffraction patterns observed for the ternary mixture revealed diffraction patterns matching those of EFV alone, as indicated with arrows. It is clear that EFV has not fully dissolved in the blend, but is partially present in a crystalline form as the saturation solubility of EFV was exceeded through use of a 60% *w/w* component for EFV in these studies. 1.4 g of EFV (58.3% *w/w*) was visually observed to be completely dissolved in 1.0 g of the 70:30 binary mixture of GM: THP.
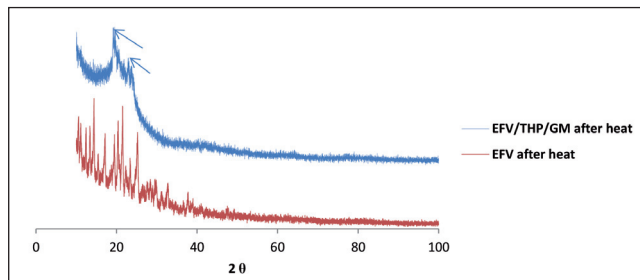
Fig. 14: WAXS pattern for the ternary mixture of EFV, GM and THP following exposure to 70 °C for one hour (blue).

## 2.3. Conclusions

EFV has been an important addition to the treatment regimen of HIV for 21 years and has significantly contributed to the emergence and evolution of HAART due to its efficacy and once-a-day dosing requirement. Despite the potent activity of EFV in the management of HIV/AIDS, the concentration of EFV in brain tissue exceeds therapeutic concentrations, leading to psychiatric effects such as severe depression and suicidal ideation. Therefore, the incorporation of EFV into SLN and/or NLC, which are lipidic may result in the potential to sustain the release of this highly lipophilic molecule and target brain tissue following oral administration, whilst reducing or limiting the incidence of adverse psychiatric effects. EFV was soluble in all solid and liquid lipids evaluated, however GM and THP exhibited the best-solubilising potential for EFV. The lipids were considered appropriate for inclusion in formulation development and manufacturing processes to produce EFV-loaded SLN and/or NLC. GM exists in the stable β-modification prior to exposure to heat, however the polymorphic form is altered to an α-modification following exposure to heat. The optimum ratio for GM and THP for the manufacture of EFV-NLC was 70:30. At this ratio the two lipids are miscible and were assumed to have the greatest solubilising potential for EFV (58.3 % w/w). DSC analysis revealed that the lipid samples had an onset of melting that is higher than the recommended temperature of 40 °C.

The addition of THP to GM resulted in the formation of a different polymorph of the solid lipid from the β-polymorphic form to one in which the α- and β'-polymorphic modifications coexist. Furthermore, the addition of a 60% w/w amount of EFV to the 70:30 binary mixture of GM and THP revealed that some of the API existed in the crystalline state within the mixture without any potential interactions between EFV and the lipids of choice.

Theoretically the relatively high solubility of EFV in THP in comparison to GM suggests that NLC are likely to have a higher EE for EFV than SLN. In addition, the co-existence of the α- and β'-polymorphic modifications of the solid lipid matrix suggests that expulsion of EFV on extended storage is unlikely to occur, if EFV is incorporated into NLC rather than SLN.

## 3. Experimental

### 3.1. Materials

EFV was donated by Adcock Ingram® Limited (Johannesburg, Gauteng, South Africa). Gelucire® 43/01 (glyceryl esters of saturated fatty acids), Compritol® 888 (glyceryl behenate) and Precirol® ATO 5 (glyceryl distearate) were donated by Gattefossé SAS (Gattefossé SAS, Saint-Priest Cedex, France). Glyceryl monostearate was purchased from Aspen® Pharmacare (Port Elizabeth, Eastern Cape, South Africa). Lauroglycol™ 90 (propylene glycol monolaurate type II), Lauroglycol™ FCC (propylene glycol monolaurate type I), Capryol™ PGMC (propylene glycol monocaprylate type I), Labrafac™ Lipophile WL1349 (medium chain triglycerides), Geloil™ SC (soya bean oil and glyceryl distearate polyglyceryl-3 dioleate), Labrasol® (caprylocaproyl macrogol-8 glycerides), Labrafac™ PG (propylene glycol dicaprylocaprate), Labrafil® M1944CS (oleoyl macrogol-6 glycerides), Transcutol® HP (diethylene glycol monoethyl ether), Capryol™ 90 (propylene glycol monocaprylate type II), Labrafil® M2125CS (linoleoyl macrogol-6 glycerides) were donated by Gattefossé SAS (Gattefossé SAS, Saint-Priest Cedex, France). All materials were used as received without further purification.

### 3.2. Screening of lipid excipients

#### 3.2.1. Selection of solid and liquid lipids

The solubility of EFV in different solid and liquid lipids was determined by dissolving increasing amounts of EFV in a fixed quantity of molten lipid and evaluation of the melt visually (Kasongo et al. 2011; Kasongo 2010). Initially 0.05 g EFV and 1.0 g of the lipid were accurately weighed using a Model PA 2102 Ohaus® top-loading analytical balance (Ohaus® Corp. Pine Brook, NJ USA) and transferred into a test tube (Pyrex® Laboratory Glassware, England). The sample was then exposed to 70 °C heat for one hour using a LABOTEC® shaking water bath (Laboratory Thermal Equipment, Greenfield NR. Oldham) set at a speed of 100 rpm. The disappearance of EFV in the molten dispersion was observed visually as an indication of the solubility of EFV in the lipid. Following solution, additional 0.05 g aliquots of EFV was added until saturation was observed and no additional EFV had dissolved after 24 hours of shaking at 70 °C in the lipid. Validity of visual inspection in these studies was confirmed by determination of solid and liquid lipids with the best solubilization potential for EFV using Hansen solubility parameter predictions as reported by our research group (Makoni et al. 2020).

#### 3.2.2. Selection of solid and liquid lipid for binary mixture

The solid and liquid lipids with the greatest solubilising capacity of EFV as identified from the studies described in 3.2.1 were mixed. Different ratios of solid and liquid lipids were tested to establish a ratio mixture that would facilitate the production of NLC (Kasongo et al. 2011). The miscibility of the two components was evaluated using a total lipid content of 1.0 g tested in ratios of solid:liquid lipid of 95:5, 90:10, 85:15, 80:20, 75:25, 70:30, 60:40, 50:50 and 40:60. Samples were weighed directly into a glass test tube and placed into a LABOTEC® shaking water bath (Laboratory Thermal Equipment, Greenfield NR. Oldham) for one hour with the temperature and speed set to 70 °C and 100 rpm, respectively. The samples were removed and cooled to room temperature (22 °C) for 24 h prior to analysis. The miscibility of the two lipids was evaluated by smearing a small sample of the dried mixture onto hydrophilic filter paper (Whatman® 110 diameter filter papers, Whatman® International Ltd, Maidstone, England) and visually inspected for the presence of oil droplets (Kasongo et al. 2011). A miscible binary mixture of lipids for which the highest solubility of EFV was expected was selected for the preparation of NLC and the melting point was determined using DSC to confirm it was > 40 °C. In addition, the maximum solubility of EFV in the selected binary mixture was identified as described in section 3.2.1.

### 3.3. Characterisation of bulk lipids

Fourier Transform Infrared Spectroscopy (FT-IR), Differential Scanning Calorimetry (DSC) and Wide-angle X-ray Scattering (WAXS) was used to characterise polymorphic modifications of bulk lipids. FT-IR characterization was performed using a Spectrum 100 Perkin-Elmer® Precisely FT-IR spectrophotometer (Perkin-Elmer® Pty Ltd, Beaconsfield, England). The scans were performed over the wavenumber range 4000 - 650 cm$^{-1}$.

DSC data was generated using a Model Q100 DSC (TA instruments, Lukens Drive New Castle, DE, USA). Samples weighing 3-5 mg were heated from 22 °C to 250 °C and consequently cooled to 22 °C at heating and cooling rates of 10 °C/min. The system was purged with liquid nitrogen at a flow rate of 100 ml/min. DSC analysis of samples prior to and after exposure to heat was an attempt to mimic conditions used during production and analysis of SLN/NLC (Kasongo et al. 2011; Müller et al. 2008).

WAXS patterns for bulk lipids were recorded using a Model D8 Discover X-ray diffractometer (Bruker, Billeria, MA, USA) equipped with a PSD LynxEye detector coupled to a copper anode (Cu-Kα radiation, λ = 1.5405 Å, 30 kV) fitted with a nickel filter. Samples were placed on a zero background silicon wafer embedded in a generic sample holder. The data were recorded at room temperature (22 °C) using a 2 θ range between 10° and 100°, a scanning rate of 1° min$^{-1}$, a filter time constant of 2.0 s per step and a slit width of 6.0 mm. Similar samples to those used to generate DSC data were used in order to simplify assessment and data analysis. The scattering angles of WAXS diffraction patterns were transformed into short spacing using Bragg's equation Eq. 1 (Mikla and Mikla 2014) to generate information about lipid modifications.

$$d = \frac{\lambda}{\sin 2\theta} \qquad (1)$$

### 3.4. Interaction of bulk lipids with EFV

Potential physical interactions between the lipids and EFV were investigated using FT-IR, DSC and WAXS as described in Section 3.3. Binary mixtures of GM and EFV in addition to a mixture of GM, THP and EFV were analysed.

Conflict of interest: None declared.

### References

Almond LM, Hoggard PG, Edirisinghe D, Khoo SH, Back DJ (2005) Intracellular and plasma pharmacokinetics of efavirenz in HIV-infected individuals. J Antimicrob Chemother 56: 738–744.

Bozal B, Uslu B, Özkan SA (2011) A review of electroanalytical techniques for determination of anti-HIV Drugs. Int J Electrochem 2011: 1–17.

Dupin N, Buffet M, Marcelin AG, Lamotte C, Gorin I, Ait-Arkoub Z, Tréluyer JM, Bui P, Calvez V, Peytavin G (2002) HIV and antiretroviral drug distribution in plasma and fat tissue of HIV-infected patients with lipodystrophy. AIDS 16: 2419–2424.

Ghasemiyeh P, Mohammadi-Samani S (2018) Solid lipid nanoparticles and nanostructured lipid carriers as novel drug delivery systems: Applications, advantages and disadvantages. Res Pharm Sci 13: 288–303.

Hou D, Xie C, Huang K, Zhu C (2003) The production and characteristics of solid lipid nanoparticles (SLNs). Biomaterials 24: 1781–1785.

Hu FQ, Jiang SP, Du YZ, Yuan H, Ye YQ, Zeng S (2006) Preparation and characteristics of monostearin nanostructured lipid carriers. Int J Pharm.314, 83–89.

Joshi M, Patravale V (2006) Formulation and evaluation of nanostructured lipid carrier (NLC)–based gel of valdecoxib. Drug Dev Ind Pharm 32: 911–918.

Kasongo KW (2010) An investigation into the feasability of incorporating didanosine into innovative solid lipid nanocarriers. PhD thesis, Rhodes University, South Africa.

Kasongo KW, Pardeike J, Müller RH, Walker RB (2011) Selection and characterization of suitable lipid excipients for use in the manufacture of didanosine-loaded solid lipid nanoparticles and nanostructured lipid carriers. J Pharm Sci 100: 5185–5196.

Makoni PA (2014) Formulation, development and assment of efavirenz-loaded lipid nanocarriers. MSc Thesis, Rhodes University, South Africa.

Makoni PA, Kasongo KW, Walker RB (2019) Short term stability testing of efavirenz-loaded solid lipid nanoparticle (SLN) and nanostructured lipid carrier (NLC) dispersions. Pharmaceutics 11: 397.

Makoni PA, Ranchhod J, WaKasongo K, Khamanga SM, Walker RB (2020) The use of quantitative analysis and Hansen solubility parameter predictions for the selection of excipients for lipid nanocarriers to be loaded with water soluble and insoluble compounds. Saudi Pharm J 28: 305–315.

Médecins Sans Frontières Access Campaign, n.d. Untangling the Web of Antiretroviral Price Reductions 15th Edition [WWW Document]. URL https://msfaccess.org/untangling-web-antiretroviral-price-reductions-15th-edition (accessed 8.8.19).

Mehnert W, Mäder K (2002) Solid lipid nanoparticles production, characterization and applications. Adv Drug Deliv Rev 47: 165–196.

Mikla VI, Mikla VV (2014) Advances in imaging from the first X-ray images. In: Mikla VI, Mikla VV: Medical Imaging Technology, Elsevier Insights, pp.1–22.

Müller RH, Mäder K, Gohla S (2000) Solid lipid nanoparticles (SLN) for controlled drug delivery- a review of the state of the art. Eur J Pharm Biopharm 50: 161–177.

Müller RH, Radtke M, Wissing S (2002) Solid lipid nanoparticles (SLN) and nanostructured lipid carriers (NLC) in cosmetic and dermatological preparations. Adv Drug Deliv Rev 54: S131–S155.

Müller RH, Radtke M, Wissing SA (2002) Nanostructured lipid matrices for improved microencapsulation of drugs. Int J Pharm 242: 121–128.

Müller RH, Runge SA, Ravelli V, Thünemann AF, Mehnert W, Souto EB (2008) Cyclosporine-loaded solid lipid nanoparticles (SLN): drug-lipid physicochemical interactions and characterization of drug incorporation. Eur J Pharm Biopharm 68: 535–544.

Puzantian T (2002) Central nervous system adverse effects with efavirenz: case report and review. Pharmacotherapy 22: 930–933.

Ravichandran S, Veerasamy R, Raman S, Krishnan N, Agrawal RK (2008) An overview on HIV-1 reverse transcriptase inhibitors. Digest J Nanomat Biostruct 3: 171–187.

Rossiter D (2016) South African Medicines Formulary, 12th ed. ed. Health and Medical Pub. Group, Claremont South Africa.

Rowe R, Sheskey P, Quinn M (2009) Handbook of pharmaceutical excipients, 6th ed. The Pharmaceutical Press, London.

Souto E, Wissing S, Barbosa C, Müller R (2004) Development of a controlled release formulation based on SLN and NLC for topical clotrimazole delivery. Int J Pharm 278: 71–77.

Souto EB, Mehnert W, Müller RH (2006) Polymorphic behaviour of Compritol®888 ATO as bulk lipid and as SLN and NLC. J Microencapsul 23: 417–433.

Souto EB, Müller RH (2011) Solid lipid nanoparticles and nanostructured lipid carriers-lipid nanoparticles for medicals and pharmaceuticals. Encycl Nanosci Nanotechnol 23: 313–328.

Taneja S, Shilpi S, Khatri K (2016) Formulation and optimization of efavirenz nanosuspensions using the precipitation-ultrasonication technique for solubility enhancement. Artif Cells Nanomed Biotechnol 44: 978–984.

UNAIDS, n.d. Global HIV &amp; AIDS statistics — 2019 fact sheet [WWW Document]. URL https://www.unaids.org/en/resources/fact-sheet (accessed 8.8.19).

Venkatesham M, Madhusudhan A, Veerabhadram G, Reddy G (2012) Design and evaluation of efavirenz loaded solid lipid nanoparticles to improve the oral bioavailability. Int J Pharm Pharm Sci 2: 84–89.

Wissing SA, Kayser O, Müller RH (2004) Solid lipid nanoparticles for parenteral drug delivery. Adv Drug Deliv Rev 56: 1257–1272.

Zimmermann E, Souto EB, Müller RH (2005) Physicochemical investigations on the structure of drug-free and drug-loaded solid lipid nanoparticles (SLN) by means of DSC and 1H NMR. Pharmazie 60: 508–513.